

## ORIGINAL ARTICLE

# Possible structural role of the disaccharide unit in Fe-bleomycin before and after oxygen activation

Teresa E Lehmann and Yang Li

Our previous investigation of the solution structure of Fe(II)-bleomycin pointed toward the carbamoyl group in the mannose moiety or a water molecule as possible alternative axial ligands to the metal center in this metallo-bleomycin. The possibility of a solvent molecule occupying the apical position *trans* to the primary amine has not been ruled out yet. In order to explore this possibility even further, the coordination chemistry of azide-bound Fe(II)-bleomycin was investigated with the use of NMR applied to paramagnetic molecules. Fe(II)- and apo-bleomycin were also re-visited. Comparison of the NMR results for both Fe(II)-bound molecules obtained in the present study strongly suggests that the carbamoyl oxygen is ligated to Fe(II), and it is released from coordination upon azide binding. This event is suggested based on the diminished paramagnetic character exhibited by the carbohydrate moiety in Fe(II)-azide-bleomycin when compared with its parent metal complex. A possible structural role for the glucopyranose fragment, which changes throughout the process that starts with metallo-bleomycin formation and ends with DNA binding, is discussed. The study of the coordination of azide by Fe(II)-bleomycin through NMR has not been reported previously. Unlike magnetic CD data, NMR offers a residue-by-residue account of the possible structural changes that take place in Fe(II)-bleomycin after azide binding.

*The Journal of Antibiotics* (2012) 65, 25–33; doi:10.1038/ja.2011.103; published online 9 November 2011

**Keywords:** antibiotic; bleomycin; coordination chemistry; glycopeptide; NMR; spectroscopy

## INTRODUCTION

Bleomycins (BLMs) (Figure 1) are antitumor agents isolated from *Streptomyces verticillus*.<sup>1</sup> Clinically, BLMs are employed for the treatment of squamous cell carcinomas,<sup>2</sup> non-Hodgkin's lymphomas,<sup>3</sup> testicular carcinomas<sup>4</sup> and ovarian cancer.<sup>5</sup> The drug acts as an antitumor agent by virtue of the ability of a metal complex of the antibiotic to cleave DNA.<sup>6–10</sup> The overall structure of this agent can be thought of as containing four distinct regions (Figure 1): the metal-binding domain, which is responsible for metal binding,<sup>11,12</sup> oxygen activation<sup>8,11,13,14</sup> and site-selective DNA cleavage,<sup>12,15</sup> the peptide linker; the DNA binding domain, containing a bithiazole moiety, which provides the majority of the DNA binding affinity,<sup>7,16</sup> and the disaccharide moiety, which may influence metal ion binding.<sup>12,17–24</sup>

With the aim of establishing structure-function correlations, much research has been devoted to the elucidation of the three-dimensional structures of some metallo-BLMs.<sup>25</sup> The results of these studies have led to the general agreement that the secondary amine of  $\beta$ -aminoalanine (A) segment, the pyrimidinylpropionamide (P) and imidazole rings, and the amide nitrogen in  $\beta$ -hydroxyhistidine (H) are the equatorial ligands to the metal centers in most of the metal-BLM adducts studied to date.<sup>25</sup> Crystal structures of Cu(II)P3-A,<sup>26</sup> Cu(II)BLM complexed with the BLM-binding protein BLMA,<sup>27</sup> and HOO-Co(III)BLM bound to DNA fragments<sup>28</sup> have pointed the primary amine in A as the endogenous axial ligand to the correspond-

ing metal centers. In the case of the ferrous complex of BLM, no crystal structure exists and there is some controversy concerning the ligation of BLM to Fe(II). Despite numerous attempts to define the endogenous ligand set in Fe(II)BLM (FeBLM), the lack of available spectroscopic techniques for high-spin ferrous systems, coupled with the complexity of the ligand framework, have made such determination very difficult. We have previously modelled the three-dimensional structures of Co(II) and Fe(II) bound BLM through NMR and molecular dynamics.<sup>18,19</sup> The results of this modelling work indicated that the most favourable structures for the aforementioned metallo-BLMs is six coordinated, with the primary amine and either the carbamoyl group in the mannose (M) moiety or a solvent molecule occupying the axial sites. Our results bolster the arguments offered by Loeb *et al.*<sup>17</sup> in their spectroscopic investigation of the metal ligation of the ferrous active site of BLM through magnetic CD (MCD).

Although a six-coordinate structure was validated by Loeb *et al.*<sup>17</sup> studies and our own NMR investigation for FeBLM, the possibility of a solvent molecule occupying the apical position *trans* to the primary amine has not been ruled out until now. To gain more insight into the possible coordination of the carbamoyl group to the Fe(II) center in FeBLM, the Fe(II)-Azide (AZ) bound BLM complex (FeAZBLM) has been studied in this work with the use of NMR. AZ is a small molecule that has been widely and successfully used to probe the dioxygen binding site in FeBLM.<sup>14,17,25</sup> Although the coordination chemistry of

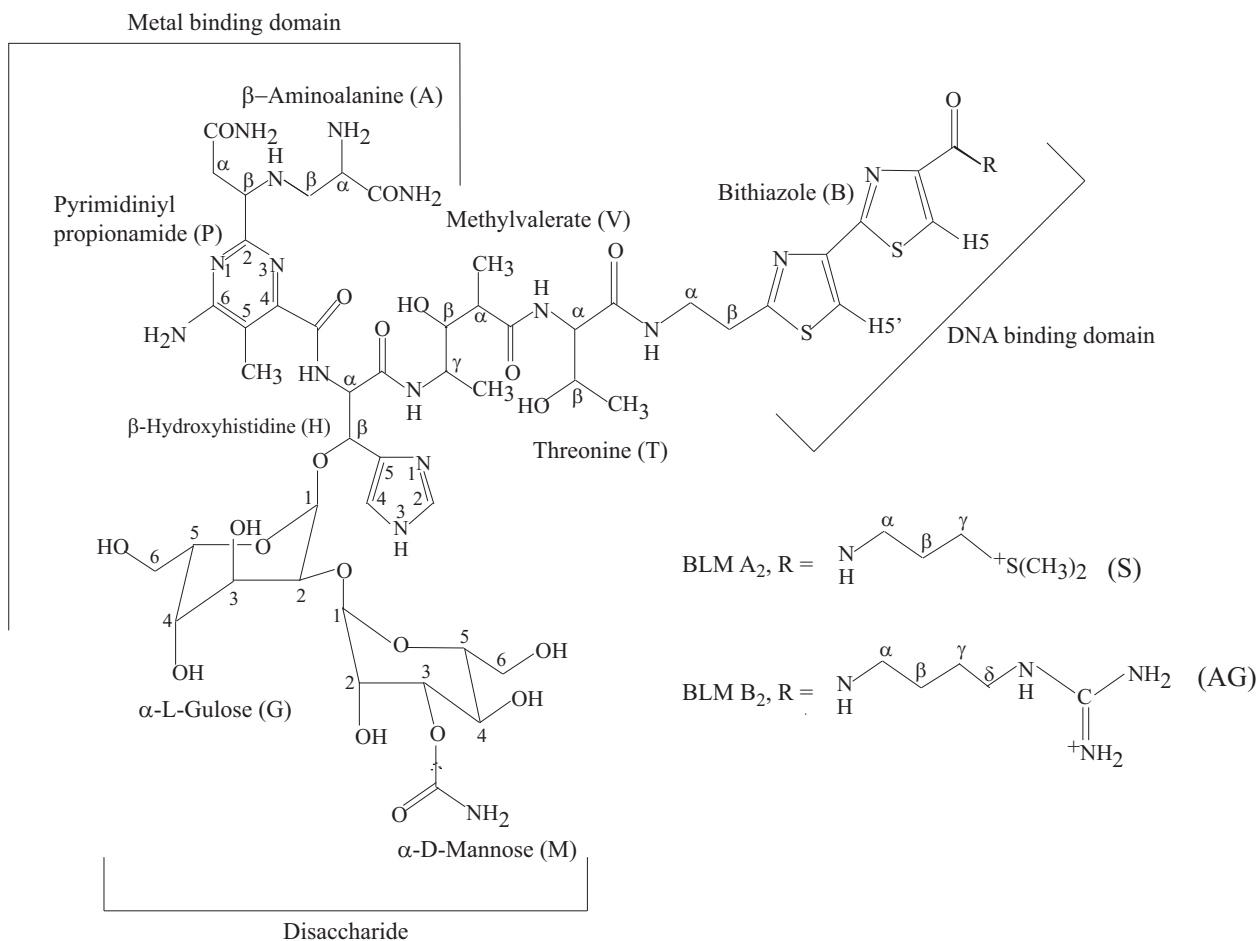


**Figure 1** Structures of BLM-A<sub>2</sub> and BLM-B<sub>2</sub>, the most abundant components in BLM.

FeBLM was assessed by us previously,<sup>24</sup> and the NMR features of the components of the BLM mixture found in bleomycin have already been assigned,<sup>29</sup> we decided to re-visit Fe- and apo-bleomycin in the present work. This is our way to ensure that the comparison between the parent and the AZ-bound molecules is done under the exact same NMR and sample preparation conditions, and to guarantee successful assignments through saturation transfer (ST) experiments. The two main NMR parameters used as the basis for the molecular comparisons discussed herein are the chemical shifts ( $\delta$ s) and the spin-lattice relaxation times ( $T_1$ s) of the protons in FeBLM and FeAZBLM. The results of the present investigation offer strong evidence pointing the carbamoyl oxygen as a ligand to the metal center in FeBLM. This conclusion is based on the diminished paramagnetic character exhibited by the carbohydrate moiety in FeAZBLM when compared with its parent metallo-BLM. These results are in agreement with the MCD studies on FeBLM and its derivatives (iso- and decarbamoyl-BLM) performed by Loeb *et al.*<sup>17</sup> In their study it was observed that upon binding of AZ, the MCD spectra of these complexes changed to an identical form, which was found consistent with the assignment of the sixth ligand as the carbamoyl substituent. Although the MCD studies referred to above have already suggested the release of the M moiety from coordination to the metal center upon addition of AZ, the NMR studies of FeAZBLM presented herein give a wider scope of the molecular changes that take place as a consequence of AZ binding, as they extend way beyond the coordination cage of the metal. Our

NMR results indicate that all BLM residues that are wrapped around the metal center in FeBLM experience molecular re-arrangement after the  $\text{N}_3^-$  ion binds to the Fe(II) center, while the BLM segment composed of the threonine (T), bithiazole (B) and ( $\gamma$ -aminopropyl)-dimethylsulfonium (S) (BLM-A<sub>2</sub>) or agmatine (AG) (BLM-B<sub>2</sub>) are less disturbed.

## RESULTS

One-dimensional spectra of 1 : 1 Fe:BLM samples of both FeBLM and FeAZBLM are shown in Figure 2. The NMR assignments of the paramagnetically shifted signals in these spectra, achieved mostly through ST experiments (Table 1), indicate that molecular re-arrangement takes place in FeBLM upon AZ binding, as evinced by the shifts of the  $^1\text{H}$  signals of FeAZBLM relative to those of the parent complex ( $\Delta\delta$ s, Table 2). The ST assignments shown in Table 1 allowed the identification of protons exhibiting  $\delta$ s in the 5 to  $-1$  p.p.m. region for both paramagnetic molecules through TOCSY and COSY correlations. Figure 3a shows that the signals at 21.18 p.p.m. (FeBLM) and 19.60 p.p.m. (FeAZBLM), assigned to the methylvalerate (V)  $\text{C}^{\gamma}\text{H}$  with ST for both molecules, display connectivity to signals at 7.94 p.p.m. (FeBLM) and 4.71 p.p.m. (FeAZBLM). These two last resonances are assigned to the  $\text{VC}^{\gamma}\text{CH}_3$  group in each molecule based on their intensities corresponding to three-proton signals. Figure 3b shows the connectivities of the signals at 6.38 p.p.m. (FeBLM) and 6.75 p.p.m. (FeAZBLM), assigned to the  $\text{TC}^{\beta}\text{H}$  proton

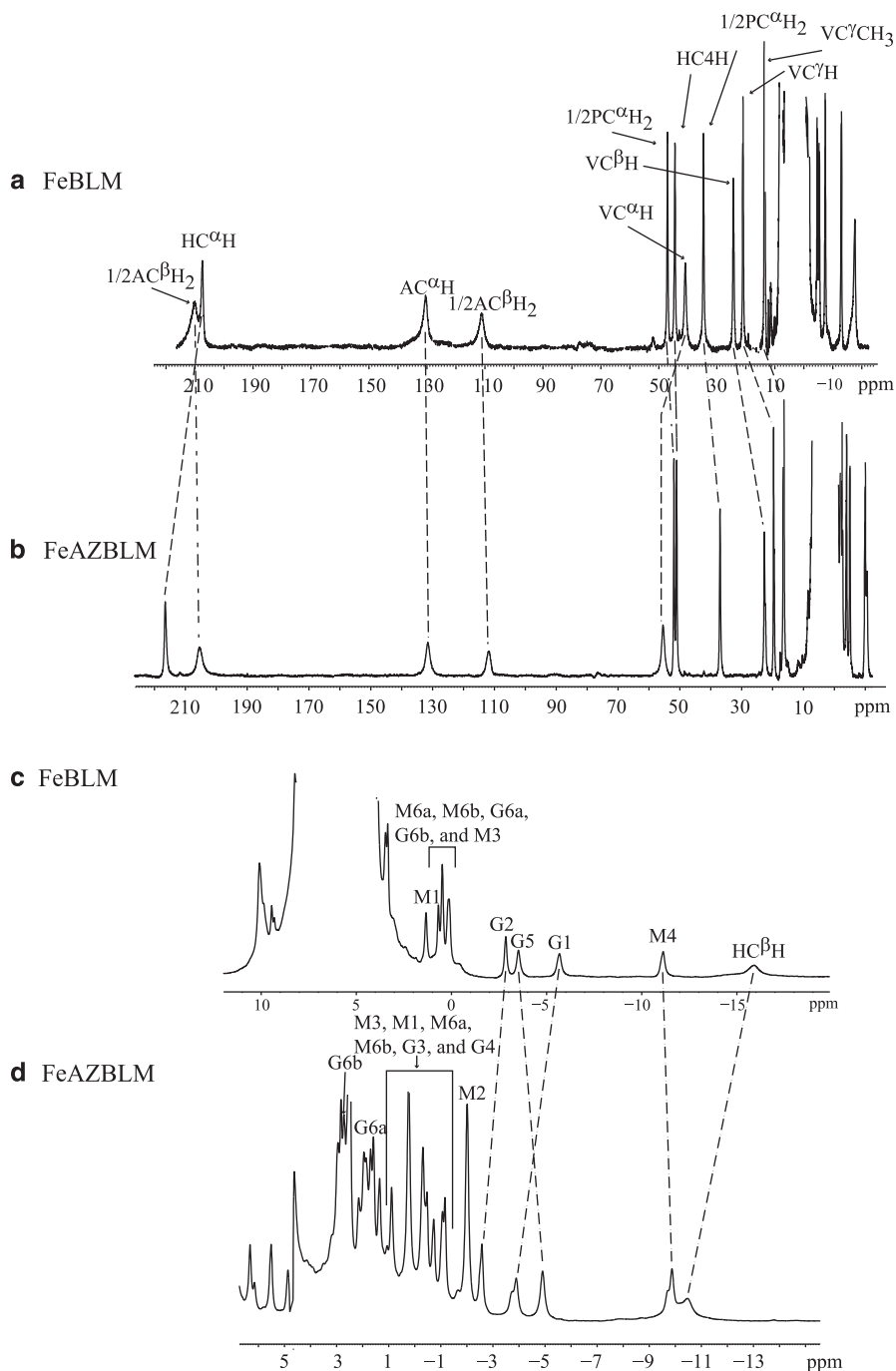


**Figure 2**  $^1\text{H}$ -NMR spectra of samples of (a) FeBLM and (b) FeAZBLM. Amplifications of the spectral regions containing the signals generated by the disaccharide fragments in (c) FeBLM and (d) FeAZBLM.

through ST, to features at 4.32 and 2.11 p.p.m. (FeBLM), and 4.77 and 2.72 p.p.m. (FeAZBLM). The intensities and positions of the latter signals led to their assignments to the  $\text{TC}^2\text{H}$  (4.32 p.p.m., FeBLM; 4.77 p.p.m., FeAZBLM) and  $\text{TCH}_3$  (2.11 p.p.m., FeBLM; 2.72 p.p.m., FeAZBLM).

Very relevant assignments are achieved through the COSY and TOCSY connectivities displayed by some of the signals of the disaccharide segment in the upfield region of the FeBLM and FeAZBLM spectra. Figures 4a and b show the 2.00 to  $-8.00$  p.p.m. and 3.00 to  $-9.90$  p.p.m. regions of TOCSY spectra collected for

FeBLM and FeAZBLM, respectively. In FeBLM the gulose (G) proton attached to the fifth carbon (G5), assigned through ST experiments, is TOCSY-correlated to another signal at  $-1.33$  p.p.m. The latter signal is in turn connected to another feature at  $-1.15$  p.p.m. as observed in TOCSY spectra collected in 90%  $\text{H}_2\text{O}/10\%$   $\text{D}_2\text{O}$  (data not shown). This network of connectivities allowed us to assign the  $-1.33$ ,  $-1.15$  p.p.m. pair to the  $\text{GCH}_2$  group in FeBLM. The M4 proton signal ( $-11.58$  p.p.m.) is correlated to a feature at  $-1.70$  p.p.m. This feature is also connected to the signal generated by the M1 proton (assigned through ST). Given the paramagnetic character of the M4

**Table 1** Saturation transfer results for FeBLM and FeAZBLM

Proton	FeBLM		FeAZBLM	
	$\delta$ (p.p.m.)	ST response (p.p.m.)	$\delta$ (p.p.m.)	ST response (p.p.m.)
HC <sup>2</sup> H	209.00 <sup>a</sup>	6.29 <sup>a</sup>	207.52	5.09
1/2AC <sup><math>\beta</math></sup> H <sub>2</sub>	201.09	2.92	194.50	2.93
AC <sup><math>\alpha</math></sup> H	123.34	3.99	122.98	3.99
1/2AC <sup><math>\beta</math></sup> H <sub>2</sub>	104.88	2.92	104.99	2.94
VC <sup><math>\alpha</math></sup> H	37.28	2.46	55.44 <sup>a</sup>	2.34 <sup>a</sup>
1/2PC <sup><math>\alpha</math></sup> H <sub>2</sub>	44.68	2.97	51.90 <sup>a</sup>	2.96 <sup>a</sup>
HC4H	42.38	7.29	51.02 <sup>a</sup>	7.32 <sup>a</sup>
1/2PC <sup><math>\alpha</math></sup> H <sub>2</sub>	32.54	2.93	34.57	2.96
VC <sup><math>\beta</math></sup> H	22.85	3.73	21.21	3.74
VC <sup><math>\gamma</math></sup> H	19.87	3.89	18.51	3.91
VC <sup><math>\alpha</math></sup> CH <sub>3</sub>	12.48	1.12	15.03	1.13
TC <sup><math>\beta</math></sup> H	6.38	4.10	6.63	4.09
G3	<sup>b</sup>	—	0.33	4.13
M1	-0.13	5.03	<sup>c</sup>	—
G4	<sup>b</sup>	—	-0.68	3.88
M2	<sup>c</sup>	—	-1.43	4.08
G1	-6.52	5.28	-3.43	5.29
G5	-4.56	4.01	-4.19	4.02
G2	-3.92	4.05	<sup>c</sup>	—
M4	-11.71	3.80	-9.09	3.82
HC <sup><math>\beta</math></sup> H	-15.98	5.92	-9.74 <sup>d</sup>	—

Abbreviation: ST, saturation transfer.

All signal positions are recorded at 303 K unless indicated otherwise.

<sup>a</sup>Measured at 293 K due to overlap with neighboring signals observed at 303 K.<sup>b</sup>Not found in the paramagnetic region.<sup>c</sup>Assigned through TOCSY correlations.<sup>d</sup>Assigned based on the results found in FeBLM for the equivalent signal.

proton signal, a connection to the M3 proton is more likely to be observed than one to the M2 proton. Additionally, the M1 proton signal is also correlated to a feature at 0.84 p.p.m. The arguments aforementioned compelled us to assign the -1.70 and 0.84 p.p.m. to M3 and M2, respectively. As the GCH<sub>2</sub> protons have already been assigned (*vide supra*), the remaining CH<sub>2</sub> group in the disaccharide region (signals at -1.46 and -1.82 p.p.m.) is assigned to the MCH<sub>2</sub> protons. The connectivities of the MCH<sub>2</sub> protons to a feature at 0.092 p.p.m. led to the assignment of the latter to the M5 proton.

For FeAZBLM, the G5 proton, assigned through ST, is clearly TOCSY-correlated to two signals (1.78 and 2.81 p.p.m.). The two latter signals are connected to each other (Figure 5b inset). This network of correlations corresponds to the G C<sub>5</sub>H-C<sub>6</sub>H<sub>2</sub> fragment. It is worth noticing that the signals arising from the GCH<sub>2</sub> protons in FeAZBLM are located in the diamagnetic region of the spectrum for this molecule, and that the G5 proton shows correlations to both GCH<sub>2</sub> protons. This situation is different from that observed for FeBLM, where G5 is only connected to one of the members of the GCH<sub>2</sub>, and the latter exhibits signals with more paramagnetic character (-1.15 and -1.33 p.p.m.). Also shown in Figure 4b is the connectivity between G1 (assigned through ST) and G2. The latter is in turn correlated to G3 and G4. The correlation between G3 and G4 was also detected in the TOCSY spectra collected for FeAZBLM. The M2 signal assigned through ST in FeAZBLM shows correlations to two signals, 1.14 and -0.13 p.p.m. COSY spectra collected for FeAZBLM at 296 K exhibit only the correlation between M2 and the -0.13 p.p.m. feature. For this reason the -0.13 p.p.m. signal is assigned to M3, and the signal at 1.14 p.p.m. is attributed to M1. The signal assigned to M4 through ST (-9.88 p.p.m.) shows a

**Table 2** Chemical shifts and T<sub>1</sub> values measured for FeBLM and FeAZBLM at 296 K

Proton	FeBLM		FeAZBLM		$\Delta\delta$ (p.p.m.) <sup>a</sup>	$\Delta T_1$ (ms) <sup>b</sup>
	$\delta$ (p.p.m.)	T <sub>1</sub> (ms)	$\delta$ (p.p.m.)	T <sub>1</sub> (ms)		
HC <sup>2</sup> H	207.43	2.95	216.56	3.09	9.13	0.14
HC <sup><math>\beta</math></sup> H	-15.92	—	-10.67	—	3.9	—
HC4H	44.75	9.86	50.84	11.13	6.09	1.27
HNH	67.16	—	—	—	—	—
1/2AC <sup><math>\beta</math></sup> H <sub>2</sub>	210.04	1.43	205.49	1.21	-4.55	-0.22
1/2AC <sup><math>\beta</math></sup> H <sub>2</sub>	111.15	0.87	109.98	0.98	-1.17	0.11
AC <sup><math>\alpha</math></sup> H	130.50	1.49	131.60	1.62	1.10	0.13
1/2PC <sup><math>\alpha</math></sup> H <sub>2</sub>	34.91	5.32	36.85	6.08	1.94	0.76
1/2PC <sup><math>\alpha</math></sup> H <sub>2</sub>	47.35	7.14	51.00	8.67	3.65	1.53
VC <sup><math>\alpha</math></sup> H	40.85	2.89	55.47	2.50	10.87	-0.39
VC <sup><math>\beta</math></sup> H	24.54	6.99	22.56	7.25	-1.98	0.26
VC <sup><math>\gamma</math></sup> H	21.18	17.19	19.60	18.20	-1.58	1.01
VC <sup><math>\alpha</math></sup> CH <sub>3</sub>	13.68	32.76	16.33	27.58	2.65	-5.18
VC <sup><math>\gamma</math></sup> CH <sub>3</sub>	7.94	—	4.71	—	-3.23	—
M1	1.34	67.62	1.14	114.98	1.66	47.36
M2	0.84 <sup>c</sup>	—	-1.88	40.51	-2.72	—
M3	-1.70 <sup>c</sup>	90.61	-0.13	170.89	1.57	80.28
M4	-11.58	9.47	-9.88	21.65	3.16	12.18
M5	0.092 <sup>c</sup>	6.86	-0.38	74.00	-0.47	67.14
M6b	-1.46 <sup>c</sup>	87.72	-0.63	128.28	0.83	40.56
M6a	-1.82 <sup>c</sup>	98.22	-0.95	103.40	0.87	5.18
G1	-5.68	11.15	-3.89	17.18	3.92	6.03
G2	-2.86	50.50	-2.42	61.17	2.27	10.67
G3	—	—	-0.23	37.71	—	—
G4	—	—	-1.05	128.89	—	—
G5	-3.52	11.22	-4.91	15.88	-0.30	4.66
G6b	-1.15 <sup>c</sup>	68.28	2.81	195.26	3.96	126.98
G6a	-1.33 <sup>c</sup>	65.95	1.78	169.93	3.11	103.98
TC <sup><math>\alpha</math></sup> H	4.32	—	4.77	—	0.45	—
TC <sup><math>\beta</math></sup> H	6.38	—	6.75	—	0.37	—
TCH <sub>3</sub>	2.11	—	2.72	—	0.61	—
TNH	15.11	—	—	—	—	—
B1'	2.45	—	3.35	—	0.9	—
B4'	2.60	—	3.39	—	0.79	—
B2'	2.92	—	3.49	—	0.57	—
B1	3.26	—	3.69	—	0.43	—
B5	2.91	—	2.23	—	-0.68	—
B6'	2.59	—	3.39	—	0.8	—
B5'	2.44	—	1.94	—	-0.5	—
B6	3.26	—	2.61	—	-0.65	—
BNH	6.45	—	7.77	—	1.32	—
SB2b	3.07	—	3.71	—	0.64	—
SB2a	2.95	—	3.67	—	0.72	—
SA2a	3.18	—	2.89	—	-0.29	—
SA2b	3.32	—	3.02	—	-0.3	—
SA2NH	6.75	—	7.75	—	1.00	—
SB2NH1	6.65	—	7.31	—	0.66	—
SB2NH2	6.63	—	7.31	—	0.68	—
SB2CNH <sub>2</sub>	5.91	—	—	—	—	—
SB2CNH <sub>2</sub> '	5.80	—	—	—	—	—

<sup>a</sup>Calculated as  $\delta(\text{FeAZBLM}) - \delta(\text{FeBLM})$ .<sup>b</sup>Calculated as  $T_1(\text{FeAZBLM}) - T_1(\text{FeBLM})$ .<sup>c</sup>Assigned at 303 K due to overlap at 296 K.

correlation to another signal at -0.38 p.p.m. Based on the assignments previously performed for the M moiety (*vide supra*), the signal at -0.38 p.p.m. is assigned to the M5 proton.

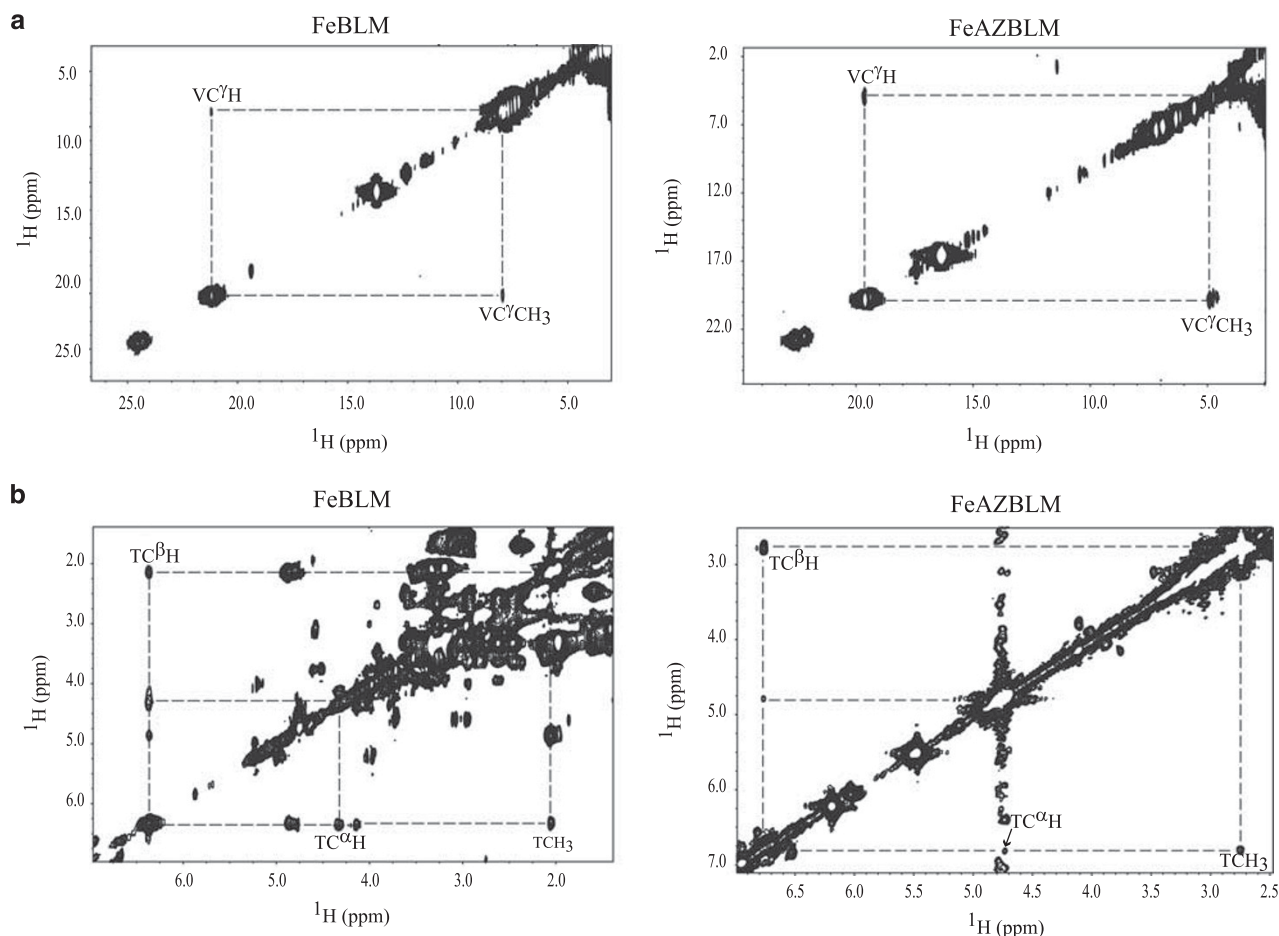


**Figure 3** (a)  $^1\text{H}$ -COSY and (b)  $^1\text{H}$ -TOCOSY spectra in  $\text{D}_2\text{O}$  of FeBLM and FeAZBLM collected at 296 K displaying the connectivities between the  $\text{VC}^\gamma\text{H}$  and  $\text{VC}^\gamma\text{CH}_3$ , and  $\text{TC}^\alpha\text{H}$ ,  $\text{TC}^\beta\text{H}$  and  $\text{TCH}_3$  signals for both molecules.

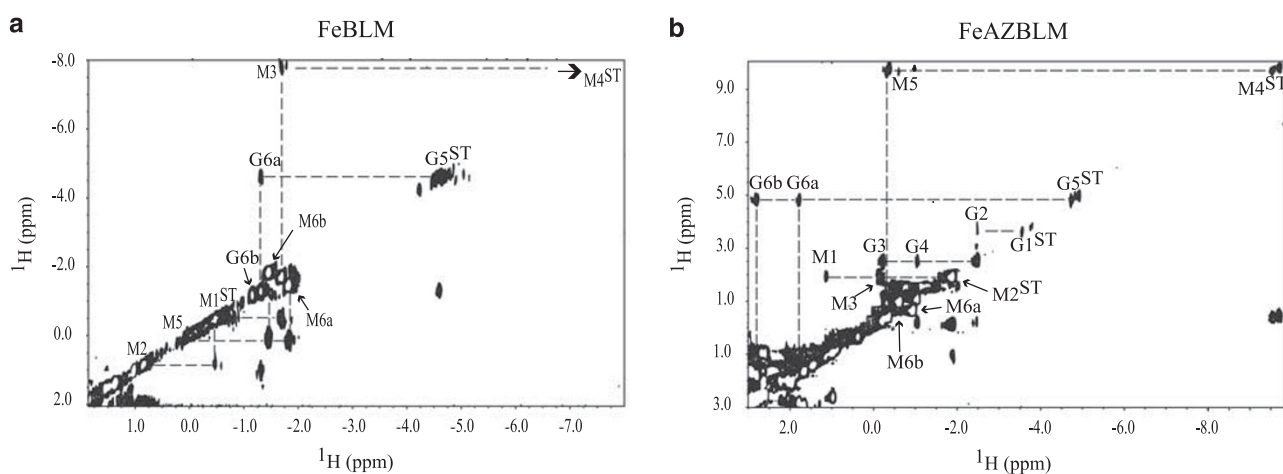


**Figure 4**  $^1\text{H}$ -TOCOSY spectra in  $\text{D}_2\text{O}$  of (a) FeBLM and (b) FeAZBLM collected at 296 K displaying the connectivities among the disaccharide protons for both molecules. The superscript (<sup>ST</sup>) has been added to some signal labels to indicate that they have been assigned through saturation transfer (ST) experiments.

The assignments performed for each molecule are collected in Table 2. As it can be seen from this table, FeAZBLM shows a richer correlation pattern for the disaccharide when compared with its parent Fe(II) complex. This result is consistent with the sugar segment

in FeBLM exhibiting a diminished paramagnetic character upon AZ binding.

Spectra collected in the diamagnetic region for FeBLM and FeAZBLM are shown in Figures 5a and b, respectively. As previously

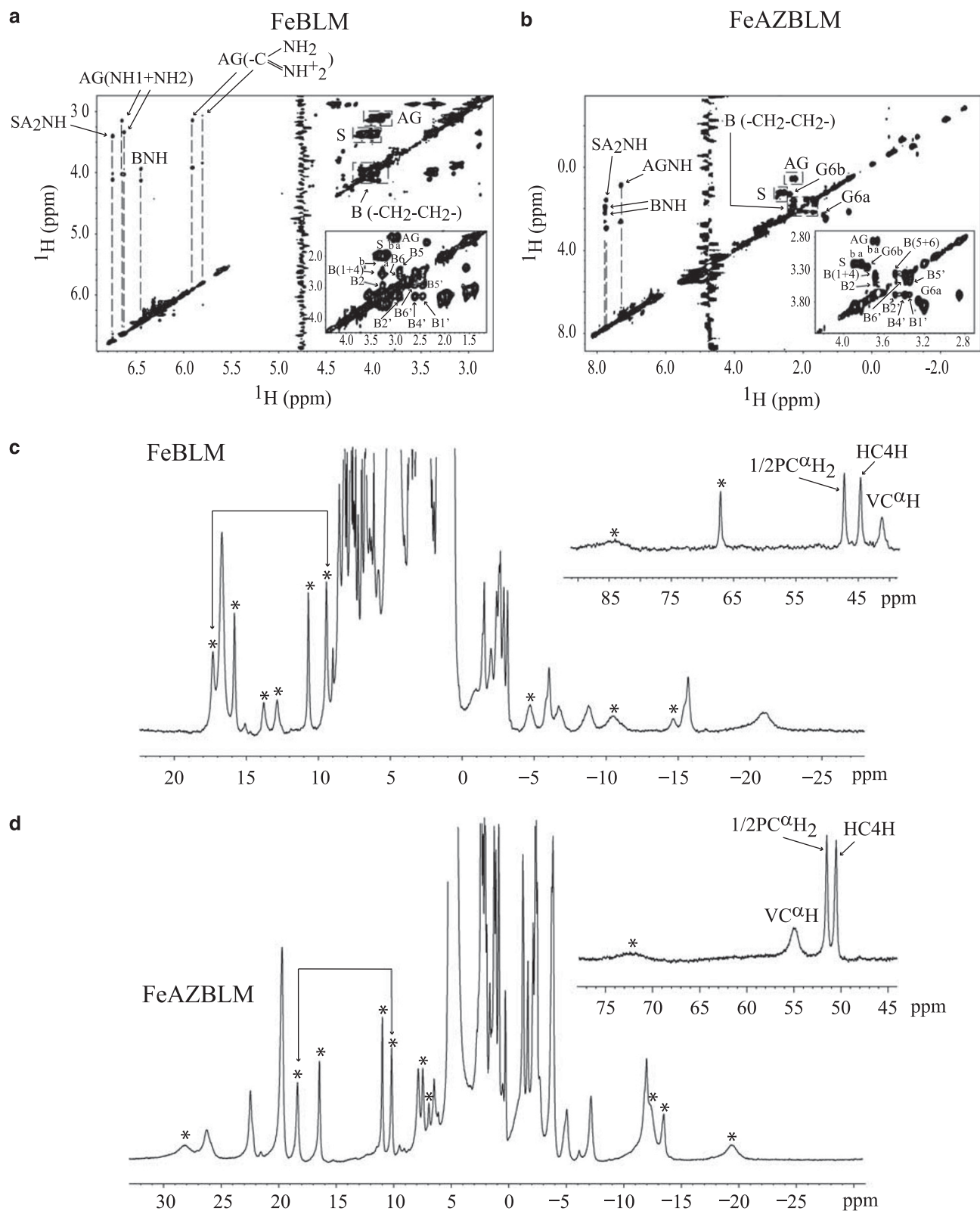


**Figure 5**  $^1\text{H}$ -TOCSY spectra in  $\text{H}_2\text{O}$  of (a) FeBLM and (b) FeAZBLM at 296 K displaying the assignments of some of the B, S and AG moieties and their NH protons. Insets:  $^1\text{H}$ -TOCSY spectra in  $\text{D}_2\text{O}$  of FeBLM and FeAZBLM at 296 K.  $^1\text{H}$ -NMR spectra of (c) FeBLM and (d) FeAZBLM in  $\text{H}_2\text{O}$  at 276 K. Asterisks (\*) are used to label the signals generated by NH protons in each spectrum. Double headed arrows are used in these spectra to connect signals arising from  $\text{NH}_2$  groups.

reported for FeBLM,<sup>24</sup> the B, AG and S protons show TOCSY and COSY correlations that allowed their assignments for both FeBLM and FeAZBLM in the present study. The signal positions for these moieties are summarized in Table 2. The diamagnetic character of these terminal BLM segments indicates that they do not participate in metal ligation, and remain rather far from the metal-binding domain in the paramagnetic molecules. The insets in Figures 5a and b are expansions of the regions of the TOCSY spectra collected on FeBLM and FeAZBLM containing the B, AG and S proton signals. Although these signals could not be assigned in detail, they are displayed, and specially labelled, in the insets, to indicate that molecular re-arrangement is also exhibited by the corresponding BLM moieties upon AZ binding.

Some NH signals were also identified for FeBLM and its AZ bound derivative (Figures 5a and b). Their assignments are reported in Table 2. The NH protons of the B, AG and S units were easily assigned for both FeBLM and FeAZBLM based on their TOCSY connectivities to some of the non-exchangeable protons in these moieties. The NH protons exhibiting hyperfine shifts (Figures 5c and d) are more difficult to identify, as they lack the aforementioned TOCSY connectivities. However, they are referred to in this study to show that they too hint molecular re-arrangement of FeBLM upon AZ binding. The double headed arrows in Figures 5c and d are connecting NH signals that show correlations to each other in TOCSY spectra collected at 276 K in H<sub>2</sub>O. These signals are generated by an NH<sub>2</sub> group in the BLM molecule. Unfortunately, the lack of TOCSY and/or COSY correlations between these signals and those of other non-exchangeable protons precluded their assignment. The insets in Figures 5c and d display parts of the 1D spectra collected for FeBLM and FeAZBLM at 296 K, and show the most paramagnetic NH protons identified for these molecules in the present study, also exhibiting different  $\delta$ s in FeBLM and FeAZBLM.

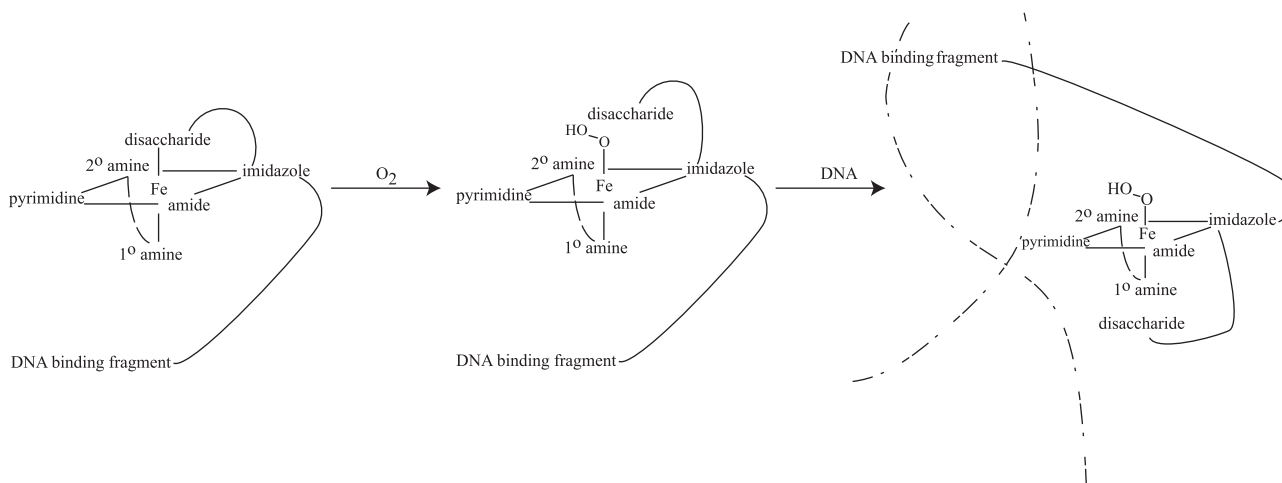
The  $T_1$ s of the protons in a molecule chelating a paramagnetic center, such as high spin Fe(II), are very good indicators of the degree of influence the metal center has on them. The  $T_1$  values for the nuclei in the A, P, H, G, M and V residues in FeBLM and its AZ-bound derivative were measured in this study and are shown in Table 2. A quick glance at the  $\Delta T_1$ s, calculated as the difference:  $T_1(\text{FeAZBLM}) - T_1(\text{FeBLM})$ , shown in Table 2 indicates that the binding of AZ lessens the paramagnetic nature of the sugar segment in FeBLM. This result is consistent with the release of the carbamoyl oxygen from coordination to the Fe(II) ion in FeBLM upon N<sub>3</sub><sup>-</sup> binding.

## DISCUSSION

As mentioned in the Results section, there are two NMR experimental outcomes from the present investigation that hint the release of the carbamoyl oxygen from coordination to the Fe(II) center in FeBLM upon AZ binding. They are the  $\Delta T_1$  and  $\Delta\delta$  values calculated as differences between the NMR signals of FeAZBLM and FeBLM (Table 2). The  $\Delta\delta$  values indicate that molecular rearrangement takes place in the FeBLM molecule upon AZ binding. The new positions of the NMR signals in FeAZBLM, which are well illustrated in Figure 2, arise from the protons in this molecule being in different chemical and/or magnetic environments when compared with the proton surroundings in FeBLM. This repositioning of the NMR signals is expected if the carbamoyl oxygen is released from coordination in FeAZBLM to allow N<sub>3</sub><sup>-</sup> binding. As seen from the  $\Delta\delta$ s displayed in Table 2, the largest values are exhibited by the A, P, H, V, M and G molecular segments, with the T, B, AG and S fragments being the least disturbed. Previous investigations on the solution

structure of various metallo-BLMs<sup>25</sup> have made it very clear that the A through V region of the BLM molecule is wrapped around the corresponding metal centers, whereas the T through S fragment is folded back underneath the equatorial plane of the metal, rather far from the metallic ion. Our results here are consistent with these facts in the form of  $\Delta\delta$ s. If the A–V segment in BLM gives the metal its niche, a change in the coordination environment of the metal center, through the binding of an exogenous ligand (N<sub>3</sub><sup>-</sup>), should translate into a structural re-shaping of the niche. It is rather difficult at this point to explain the magnitude and sign of each  $\Delta\delta$ . An NMR-derived three-dimensional solution structure of FeAZBLM and its comparison with that for FeBLM<sup>18</sup> would be very useful to this end. Structural calculations are underway in our lab to achieve such a goal.

The  $T_1$  values of protons close to the metal center in a paramagnetic molecule are very important to determine their proximity to it. The interactions between magnetic nuclei in a paramagnetic molecule and the unpaired electrons from the metal center can be separated in two contributions: spin density at the resonating nucleus (Fermi contact coupling), and the spin density cloud in the rest of the molecule (through-space dipolar coupling).<sup>30,31</sup> Spin density near a resonating nucleus is always relatively small, and therefore it has a significant contribution only for nuclei at small distances from the paramagnetic center. In FeBLM only protons very close to a metal ligating site, such as those in the A, P and H moieties, exhibit significant Fermi contact interactions, which mostly generates their large downfield  $\delta$ s and very short  $T_1$ s<sup>24</sup> (Figure 2 and Table 2). Dipolar interactions account, for example, for the paramagnetic behaviour of the protons in the V residue. As the disaccharide unit in BLM binds the metal center through its carbamoyl oxygen, it is expected that the protons in this unit experience mostly dipolar interactions with the Fe(II) center, which explain their milder upfield paramagnetic features and longer  $T_1$ s. The  $T_1$  and  $\delta$  values of the protons in the disaccharide BLM fragment in FeBLM and its AZ-bound derivative indicate that the sugar segment in both molecules displays paramagnetic behaviour. However, longer relaxation times, indicative of larger metal-to-proton distances, were measured for these protons in FeAZBLM (Table 2). This result suggests that after detaching from the Fe(II) center in FeBLM upon AZ binding, the disaccharide fragment still remains in the vicinity of the coordination cage in FeAZBLM. This outcome is not surprising if considered in light of the crystal structure of HOO-Co(III)BLM bound to a DNA fragment.<sup>28,32</sup> In this crystal structure the metal-binding domain and disaccharide moieties partially stack against each other and display base-specific hydrogen bonding to each respective wall of the DNA minor groove. The M carbamoyl amide and its C–OH form hydrogen bonds with the DNA bases that are very important for the stabilization of the HOO-Co(III)BLM-DNA complex. Based on these results the authors propose that the glucopyranose moiety serves as a space-filling unit allowing the metal-binding domain to adopt an optimized and stabilized orientation relative to the target. If the G–M segment of BLM is to partially stack with the metal-binding domain upon DNA binding, it makes sense that it remains in the vicinity of the metal after its release from coordination. The results of the present investigation, together with those from our previous studies on FeBLM,<sup>18,24</sup> suggest that it is possible that the role of the disaccharide moiety in BLM changes as the process that involves metallo-BLM formation, oxygen activation and DNA binding and cleavage follows its course. A possible scheme of events with different roles for the glucopyranose fragment could be: (1) initial weak binding of the carbamoyl to the deoxygenated Fe(II) center assists BLM in its competition for an effective sequestration of intracellular iron before a ligand structural reorganization and oxygenation; (2) in the presence



**Scheme 1** Possible roles of the disaccharide unit in BLM.

of oxygen, the carbamoyl group is released from coordination to allow  $O_2$  binding and activation; (3) after  $O_2$  binding, the role of the disaccharide unit is that of stabilizing the metallo-BLM–DNA complex through space-filling and hydrogen bonding (Scheme 1).

The NMR data presented in this investigation strongly support the coordination of the carbamoyl oxygen in M to the metal center in FeBLM, and its release from coordination upon AZ binding. Unlike MCD data, NMR offers a residue-by-residue account of the possible structural changes that take place in FeBLM after  $N_3^-$  binding in the form of  $\Delta\delta$ s and  $\Delta T_{1s}$  (Table 2). The NMR results presented in this report suggest that the binding of AZ to the metal center in FeBLM alters the whole molecular structure of this metallo-BLM. However, our NMR results cannot be solely used to definitively rule out the possibility of a solvent molecule occupying one of the axial positions in the coordination cage instead of the M carbamoyl oxygen. Solution structure calculations, based on the NMR data collected for FeAZBLM and considering both coordination possibilities to fit the NMR results, are required to determine the identity of the axial ligand still subject to controversy. These calculations are underway in our lab, and they will help translate our NMR data into a reliable structure for FeAZBLM. Coordination chemistry studies and solution structure calculations of Fe(II) complexes of other mannose-modified BLMs such as iso-, decarbamoyl- and deglyco-BLM free in solution and in the presence of DNA fragments, which are also underway in our lab, will help to better establish the possible changing role of the sugar fragment of BLM in the entire process of BLM action.

## MATERIALS AND METHODS

### NMR sample preparation

Blenoxane, the commercial mixture of bleomycin congeners, was purchased from Sigma-Aldrich (St Louis, MO, USA). The commercial drug consists predominantly of  $\sim 70\%$  BLM- $A_2$  and  $\sim 30\%$  BLM- $B_2$  with trace amounts of other congeners. Most of the proton resonances are identical for BLM- $A_2$  and BLM- $B_2$ , and evidence from chemical shifts studies suggests similar conformational characteristics for these two congeners.<sup>29</sup> For these reasons, blenoxane was used in the experiments without further purification and is referred to as BLM. Additionally, we are particularly interested in the properties of the clinically employed mixture of BLMs. All Fe(II)-containing samples were prepared under strict oxygen free conditions with the use of a vacuum line and an anaerobic chamber. All solids and liquids to be used in sample preparations were degassed through 15 6-min-vacuum/nitrogen cycles. For the FeBLM samples, BLM,  $6.5\ \mu\text{mol}$ , lyophilized three times from  $D_2O$  was dissolved in  $545\ \mu\text{l}$  of  $D_2O$  (99.9% d, Sigma-Aldrich). A  $200\ \text{mM}$  solution of

$\text{FeSO}_4 \cdot 7H_2O$  in  $D_2O$  was added to the initial BLM solutions to afford Fe(II):BLM ratios of 1 : 1 and 1 : 2. Subsequently,  $50\ \mu\text{l}$  of  $200\ \text{mM}$  sodium dithionite in  $D_2O$  was added to each sample. The pH was carefully adjusted to 6.5 with a  $1\ \text{M}$  NaOD solution. Visually, the colorless solution of BLM turned a pale salmon-pink color upon addition of Fe(II). The 1 : 2 and 1 : 1 Fe(II):BLM samples were transferred to purged NMR tubes, which were immediately flame-sealed. A 1 : 1 Fe(II):BLM sample in  $H_2O$  was prepared by an analogous procedure. A set of FeAZBLM samples with Fe(II):BLM ratios of 1 : 1 and 1 : 2 were prepared by a procedure similar to the one used for the FeBLM samples. Sodium AZ ( $\text{NaN}_3$ , Sigma-Aldrich) in the form of a  $4.3\ \text{M}$  solution in  $D_2O$  was added to the FeBLM samples to give  $N_3^-$  to Fe(II)<sub>M</sub> ratios of 43 : 1. Loeb *et al.*<sup>17</sup> determined the requirement of 43 M equivalents of  $\text{NaN}_3$  to prepare FeAZBLM samples in their MCD studies of ferrous BLM. Visually, the salmon-pink FeBLM solution turned a watermelon-pink colour upon addition of AZ. Samples of apo-BLM were prepared by dissolving  $6.5\ \mu\text{M}$  of BLM in  $650\ \mu\text{l}$  of  $H_2O$  and  $D_2O$ . The pH of the apo-BLM samples was also adjusted to 6.5.

### NMR spectra

NMR experiments were performed at 400 MHz on a Bruker DRX-400 NMR spectrometer (Bruker Corporation, Billerica, MA, USA). All chemical shifts were referenced to HDO as the internal standard. The solvent signal was irradiated in all spectra. The one-dimensional (1D) spectra were obtained using a  $7\text{-}\mu\text{s}$   $90^\circ$  pulse with 32 K data points. Signal-to-noise ratios were improved by applying a line-broadening factor of 20 Hz to the free-induction-decay (FID) before FT. An inversion-recovery pulse sequence was used to obtain nonselective  $T_{1s}$ , with the carrier frequency set at three different positions to ensure the validity of the measurements.

$ST^{30}$  experiments were performed on the 1 : 2 Fe:BLM and AZ-bound 1 : 2 Fe:BLM samples in  $D_2O$ , using a 1-D nuclear Overhauser experiment<sup>33</sup> pulse sequence. A 70 ms irradiation time was used for all paramagnetic signals. Due to the differences in  $T_{1s}$  exhibited by the FeBLM protons located in different regions of the 1D spectra (Figure 2), the following irradiation powers were used in the ST experiments: signals in the 220–100 p.p.m. region, 30 db; signals between 50 and 13, and –3 and –17 p.p.m., 50 db; signals between –0.8 and –3.5 p.p.m., 70 db. The ST responses were determined from difference spectra, obtained by subtracting the spectra, where the signals are irradiated from spectra with the decoupler located at neutral positions. Most of the ST experiments were performed at 303 K unless indicated otherwise. Spin-echo correlated spectroscopy (SECSY)<sup>34</sup> experiments were performed on apo-BLM samples in  $D_2O$  at 303 K to be used as references for the signal positions in the diamagnetic molecules, and properly assign the responses of the paramagnetic signals in FeBLM and FeAZBLM in the ST experiments. Before the standard SECSY pulse sequence, during the relaxation delay period (3 s), the HDO feature was selectively irradiated (40 db). Quadrature detection was used in both directions. For each value of  $t_1$ , 64 FIDs (2000 data points, acquisition



time 0.314 s) were acquired. Before FT, the FIDs were multiplied with a sine-bell window function in both directions. Spectra were calculated in absolute value mode.

Magnitude mode COSY<sup>35</sup> experiments on FeBLM and FeAZBLM covering the 50 to -20 p.p.m. region were performed at 296 and 303 K with 256 points in the  $t_2$  and  $t_1$  dimensions, a spectral width of 56 kHz, and a relaxation delay of 300 ms. COSY spectra spanning the 0–15 p.p.m. regions were acquired with 2048 points in  $t_2$  and 512 points in  $t_1$ , a spectral width of 23 kHz and a relaxation delay of 2 s. COSY spectra in water were also collected for FeBLM and FeAZBLM at 296 and 276 K in order to identify the exchangeable protons in these molecules. For these spectra, 1024 points in  $t_2$  and 512 points in  $t_1$  were acquired with spectral widths of 54 and 39 kHz and relaxation delays of 300 ms and 2 s, respectively. A zero-degree-shifted sine bell was applied before FT.

TOCSY<sup>36,37</sup> data on FeBLM and FeAZBLM both in D<sub>2</sub>O and H<sub>2</sub>O were collected at 276, 296 and 303 K. Spectra were acquired with 1024 points in  $t_2$  and 512 points in  $t_1$ , spectral widths of 56 and 23 kHz and relaxation delays of 300 ms and 2 s, respectively. A mixing time of 40 ms was used in all TOCSY spectra. A 60°-shifted sine-squared bell was applied to both dimensions before FT.

Processing and analysis of the NMR data were performed on a PC Core 2 Duo workstation using NMRPipe<sup>38</sup> and NMRView<sup>39</sup> software.

## ACKNOWLEDGEMENTS

This work was supported by the University of Wyoming start-up funds. We thank Dr Douglas Wheeler (University of Wyoming, Department of Chemistry) for his assistant with some of the NMR spectra collected during this investigation. Our gratitude also goes to Dr Vladimir Alvarado (University of Wyoming, Department of Petroleum and Chemical Engineering), for reviewing this manuscript. Our gratitude also goes to Dr Bruce A Johnson (Merck Research Laboratories, Rahway, NJ, USA) and Dr Frank Delaglio (Software Science Consultant, North Potomac, MD, USA) for kindly providing the software NMRPipe and NMRView, respectively.

- 1 Umezawa, H., Maeda, K., Takeuchi, T. & Okami, Y. New antibiotics bleomycin A and B. *J. Antibiot.* **19**, 200–209 (1966).
- 2 Bennett, J. M. & Reich, S. D. Bleomycin. *Ann. Inter. Med.* **90**, 945–948 (1979).
- 3 Carlson, R. W., Sikic, B. I., Turbow, M. M. & Ballon, S. C. Combination cisplatin, vinblastine, and bleomycin chemotherapy (PVB) for malignant germ-cell tumors of the ovary. *J. Clin. Oncol.* **1**, 645–651 (1983).
- 4 *Bleomycin Chemotherapy* (eds Sikic, B. I., Rozenzweig, M., & Carter, S. K.) Academic Press, Orlando, FL, 1985.
- 5 Einhorn, L. H. & Donohue, J. Cis-diamminedichloroplatinum, vinblastine, and bleomycin combination chemotherapy in disseminated testicular cancer. *Ann. Inter. Med.* **87**, 293–298 (1977).
- 6 Sausville, E. A., Peisach, J. & Horwitz, S. B. Role for ferrous ion and oxygen in degradation of DNA by bleomycin. *Biochem. Biophys. Res. Commun.* **73**, 814–822 (1976).
- 7 Hecht, S. M. RNA degradation by bleomycin, a naturally-occurring bioconjugate. *Bioconjugate Chem.* **5**, 513–526 (1994).
- 8 Kane, S. A. & Hecht, S. M. Polynucleotide recognition and degradation by bleomycin. *Prog. Nucleic Acid Res. Mol. Biol.* **49**, 313–352 (1994).
- 9 Hecht, S. M. Bleomycin: new perspectives on the mechanism of action. *J. Nat. Prod.* **63**, 158–168 (2000).
- 10 Chen, J. Y. & Stubbe, J. Bleomycins: towards better therapeutics. *Nat. Rev. Cancer* **5**, 102–112 (2005).
- 11 Boger, D. L. & Cai, H. Bleomycin: synthetic and mechanistic studies. *Angew. Chem. Int. Ed.* **38**, 448–476 (1999).
- 12 Carter, B. J., Murty, V. S., Reddy, K. S., Wang, S. -N. & Hecht, S. M. A role for the metal-binding domain in determining the DNA-sequence selectivity of Fe-bleomycin. *J. Biol. Chem.* **265**, 4193–4196 (1990).
- 13 Hecht, S. M. The chemistry of activated bleomycin. *Acc. Chem. Res.* **19**, 383–391 (1986).
- 14 Stubbe, J. & Kozarich, J. W. Mechanisms of bleomycin-induced DNA-degradation. *Chem. Rev.* **87**, 1107–1136 (1987).
- 15 Povirk, L. F., Hogan, M. & Dattagupta, N. Binding of bleomycin to DNA - intercalation of the bithiazole rings. *Biochemistry* **18**, 96–101 (1979).
- 16 Zuber, G., Quada, J. C. & Hecht, S. M. Sequence selective cleavage of a DNA octanucleotide by chlorinated bithiazoles and bleomycins. *J. Am. Chem. Soc.* **120**, 9368–9369 (1998).
- 17 Loeb, K. E., Zaleski, J. M., Hess, C. D., Hecht, S. M. & Solomon, E. I. Spectroscopic investigation of the metal ligation and reactivity of the ferrous active sites of bleomycin and bleomycin derivatives. *J. Am. Chem. Soc.* **120**, 1249–1259 (1998).
- 18 Lehmann, T. E. Molecular modeling of the three-dimensional structure of Fe(II)-bleomycin: are the Co(II) and Fe(II) adducts isostructural? *J. Biol. Inorg. Chem.* **7**, 305–312 (2002).
- 19 Lehmann, T. E., Serrano, M. L. & Que, L. Jr. Coordination chemistry of Co(II)-bleomycin: Its investigation through NMR and molecular dynamics. *Biochemistry* **39**, 3886–3898 (2000).
- 20 Akkerman, M. A. J., Neijman, E.W.J.F., Wijmenga, S. S., Hilbers, C. W. & Bermel, W. Studies of the solution structure of the bleomycin-A2 iron(II) carbon-monoxide complex by means of 2-dimensional NMR-spectroscopy and distance geometry calculations. *J. Am. Chem. Soc.* **112**, 7462–7474 (1990).
- 21 Akkerman, M. A. J., Haasnoot, C. A. G., Pandit, U. K. & Hilbers, C. W. Complete assignment of the C-13 NMR-spectra of bleomycin-A2 and its zinc complex by means of two-dimensional NMR-spectroscopy. *Magn. Reson. Chem.* **26**, 793–802 (1988).
- 22 Akkerman, M. A. J., Haasnoot, C. A. G. & Hilbers, C. W. Studies of the solution structure of the bleomycin-A2 zinc complex by means of two-dimensional NMR-spectroscopy and distance geometry calculations. *Eur. J. Biochem.* **173**, 211–225 (1988).
- 23 Oppenheimer, N. J., Rodriguez, L. O. & Hecht, S. M. Structural studies of active complex of bleomycin - assignment of ligands to the ferrous ion in a ferrous-bleomycin carbon monoxide complex. *PNAS* **76**, 5616–5620 (1979).
- 24 Lehmann, T. E., Ming, L.-J., Rosen, M. E. & Que, L. Jr. NMR studies of the paramagnetic complex Fe(II)-bleomycin. *Biochemistry* **36**, 2807–2816 (1997).
- 25 Claussen, C. A. & Long, E. C. Nucleic acid recognition by metal complexes of bleomycin. *Chem. Rev.* **99**, 2797–2816 (1999).
- 26 Iitaka, Y. *et al.* Chemistry of bleomycin 20. X-ray structure determination of P-3A Cu(II)-complex, a biosynthetic intermediate of bleomycin. *J. Antibiot.* **31**, 1070–1072 (1978).
- 27 Masanori, S., Takanori, K., Minoru, H., Masafumi, M. & Yasuyuki, M. The 1.6 Å crystal structure of the copper(II)-bound bleomycin complexed with the bleomycin-binding protein from bleomycin-producing *Streptomyces verticillus*. *J. Biol. Chem.* **277**, 2311–2320 (2002).
- 28 Goodwin, K. D., Lewis, M. A., Long, E. C. & Georgiadis, M. M. Crystal structure of DNA-bound Co(III)-bleomycin B-2: Insights on intercalation and minor groove binding. *PNAS* **105**, 5052–5056 (2008).
- 29 Chen, D. M., Hawkins, B. L. & Glickson, J. D. Proton nuclear magnetic-resonance study of bleomycin in aqueous-solution - assignment of resonances. *Biochemistry* **16**, 2731–2738 (1977).
- 30 Bertini, I., Luchinat, C. & Parigi, G. Solution NMR of Paramagnetic Molecules. *Applications to Metallobiomolecules and Models*, in *Current Methods in Inorganic Chemistry*, Vol. 2 (Elsevier, New York, 2001).
- 31 Ming, L.-J. In Nuclear magnetic resonance of paramagnetic metal centers in proteins and synthetic complexes in physical methods in bioinorganic chemistry. *Spectroscopy and Magnetism* (ed Que, L., Jr.) 375–464 University Science Books, Sausalito, California, 2000.
- 32 Long, E. C., Georgiadis, M. M., Goodwin, K. D. & Lewis, M. A. in *Bioinorganic Chemistry: Cellular Systems & Synthetic Models. ACS Symp. Series* Vol. 1012 (eds Long, E. C. & Baldwin M. J.) 63–80 (ACS, Washington, D. C., 2009).
- 33 Nehaus, D. & Williamson, M. in *The Nuclear Overhauser Effect in Structural and Conformational Analysis* (VCH Publishers, New York, 1989).
- 34 Nagayama, K., Wüthrich, K. & Ernst, R. R. 2-Dimensional spin-echo correlated spectroscopy (SECSY) for H-1-NMR studies of biological macromolecules. *Biochem. Biophys. Res. Commun.* **90**, 305–311 (1979).
- 35 Rance, M. *et al.* Improved spectral resolution in COSY H1-NMR spectra of proteins via double quantum filtering. *Biochem. Biophys. Res. Commun.* **117**, 479–485 (1983).
- 36 Braunschweiler, L. & Ernst, R. R. Coherence transfer by isotropic mixing - application to proton correlation spectroscopy. *J. Magn. Reson.* **53**, 521–528 (1983).
- 37 Bax, A. & Davis, D. G. MLEV-17-based two-dimensional homonuclear magnetization transfer spectroscopy. *J. Magn. Reson.* **65**, 355–360 (1985).
- 38 Delaglio, F. *et al.* NMRPipe - a multidimensional spectral processing system based on Unix pipes. *J. Biomol. NMR* **6**, 277–293 (1995).
- 39 Johnson, B. A. & Blevins, R. A. NMR view - a computer-program for the visualization and analysis of NMR data. *J. Biomol. NMR* **4**, 603–614 (1994).